

# Distributional fixed point equations for island nucleation in one dimension: a retrospective approach for capture zone scaling

P. A. Mulheran,<sup>1, a)</sup> K. P. O'Neill,<sup>2, b)</sup> M. Grinfeld,<sup>2, c)</sup> and W. Lamb<sup>2, d)</sup>

<sup>1)</sup>Department of Chemical and Process Engineering, University of Strathclyde, Glasgow

<sup>2)</sup>Department of Mathematics and Statistics, University of Strathclyde, Glasgow

(Dated: 27 February 2012)

The distribution of the capture zones of point islands nucleated in one dimension are considered using a retrospective view, providing an alternative perspective on why scaling occurs in this continuously evolving system. Distributional fixed point equations for the capture zones are derived through a mean field approximation for nearest neighbour size correlation. Solutions of these equations compare favourably to Monte Carlo data for a range of critical island size  $i = 0, 1, 2, 3$ , and to theoretical models based on more traditional fragmentation theory approaches.

PACS numbers: 81.15.Aa, 68.55.A-, 05.10.Gg

Keywords: Gap size distribution, capture zone distribution

Scale invariance during the nucleation and growth of islands driven by monomer deposition is an intriguing phenomenon<sup>1</sup>. Island size distributions, and the distribution of capture zones which underlie the island growth rates, evolve towards scaling forms despite on-going nucleation of new islands with the concomitant disruption to the existing capture zones<sup>2</sup>. The form of the scaling functions depends on the critical island size  $i$ , where  $i + 1$  is the smallest stable island size. A number of theoretical approaches have been used to model this behaviour, ranging from mean field models which neglect the variation in capture zone sizes<sup>3-8</sup> due to spatial arrangements of the islands, to those which attempt to include this information explicitly<sup>9-13</sup>. All these approaches can be characterised as forward-looking in the sense that they are based on predicting how size distributions evolve as new islands nucleate. In this paper we shall present an alternative, retrospective, perspective where we ask how the capture zones present in the system came to be created. We focus on the case of point island nucleation in a one dimensional (1-D) system since this allows for a more complete analysis and comparisons with results from a more traditional fragmentation theory approach<sup>14,15</sup>. This new perspective provides interesting insight into why scaling occurs and compares well with simulation data.

Island nucleation and growth is widely studied using Monte Carlo (MC) simulation. A point island approximation is often used both for clarity and because it approximates the growth of small, well-separated islands<sup>4</sup>. Here we employ a 1-D model<sup>14</sup> where monomers are deposited at random onto an initially empty lattice at a deposition rate of  $F$  monolayers per unit time. The

monomers diffuse at rate  $D$  on the lattice, nucleating immobile point islands when  $i + 1$  monomers coincide at a lattice site. Once nucleated, the islands grow by absorbing any monomers that hit them, although they only occupy one lattice site. When sufficient islands have been nucleated, the most likely fate of a deposited monomer is to become absorbed by an existing island rather than being incorporated into a new island. It is in this aggregation regime of growth where scale invariance is found; note however that island nucleation continues still, albeit at a slow rate compared to monomer adsorption.

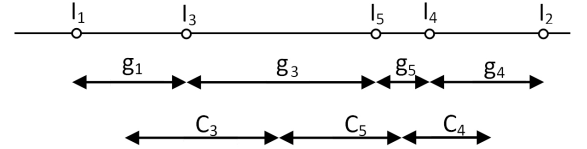


FIG. 1. The islands numbered  $I_1 - I_5$  on the one dimensional substrate. The gaps between the islands are labelled  $g_1, g_3, g_5$  and  $g_4$ , and the capture zones of islands  $I_3, I_5, I_4$  are labelled  $C_3, C_5$  and  $C_4$  respectively.

Figure 1 shows some islands on the lattice, numbered according to their chronological age, along with their capture zones  $C_3, C_4$  and  $C_5$ . Island  $I_3$  has the capture zone of size  $C_3 = (g_1 + g_3)/2$ , where  $g_1$  and  $g_3$  are the inter-island gaps to the left and right of  $I_3$  respectively.  $C_3$  represents the average growth rate of  $I_3$ , since any monomers deposited into  $C_3$  are more likely to diffuse to  $I_3$  than its neighbours  $I_1$  and  $I_5$ .

Referring to Figure 1, let us ask how the inter-island gap  $g_3$  was created. It was formed by the nucleation of the youngest island in the picture,  $I_5$ , which occurred in the gap of size  $(g_3 + g_5)$  between islands  $I_3$  and  $I_4$ . Generalising, we will suppose that any randomly chosen

<sup>a)</sup>Electronic mail: paul.mulheran@strath.ac.uk

<sup>b)</sup>Electronic mail: kenneth.o-neill@strath.ac.uk

<sup>c)</sup>Electronic mail: m.grinfeld@strath.ac.uk

<sup>d)</sup>Electronic mail: w.lamb@strath.ac.uk

gap with size  $x$  (scaled to the average) in the system will have arisen by the fragmentation of a larger gap formed by combining it with a neighbouring gap of size  $y$ . In general we do not have the benefit of the chronological ages to guide us, so we make a mean field approximation for the size of the neighbouring gap, namely  $y = 1$ . Denoting the probability of fragmenting a gap into proportions  $a$  and  $(1 - a)$  by  $P(a)$ , we find the following distributional fixed point equation (DFPE) for the probability distribution function  $\phi(x)$  of gaps  $x \in [0, \infty)$ :

$$x \triangleq a(1 + x). \quad (1)$$

This convenient notation (exploited below) states that the distribution of the variates on the left is equal to that on the right<sup>16</sup>. The DFPE leads to the Integral Equation (IE) for  $\phi(x)$ ,

$$\phi(x) = \int_0^1 \phi\left(\frac{x}{a} - 1\right) \frac{P(a)}{a} da \quad (2)$$

where we assume that  $\phi(x) = 0$  if  $x < 0$ .

This equation states that the statistical distribution of gaps is unchanged by the fragmentation of all the gaps incremented in scaled size by one. Note that we neglect long-range chronological effects here, of the type apparent in Figure 1 for the creation of gap  $g_4$  which arose from the nucleation of island  $I_4$  and the fragmentation of gap  $(g_3 + g_5 + g_4)$ . We will return to this point below.

In the aggregation regime, the probability  $P(a)$  of fragmenting a gap into proportions  $a$  and  $(1 - a)$  is found from the steady-state monomer density profile<sup>14</sup>:

$$P(a) = \frac{a^\alpha (1 - a)^\alpha}{B(\alpha + 1, \alpha + 1)} = \frac{(2\alpha + 1)!}{(\alpha!)^2} a^\alpha (1 - a)^\alpha. \quad (3)$$

Here  $B(m, n) = (m - 1)!(n - 1)!/(m + n - 1)!$  is the Beta function and  $\alpha$  reflects the dominant nucleation mechanism. For nucleation triggered by deposition of monomers,  $\alpha = i$  for  $i = 1, 2, 3 \dots$ , whereas for nucleation resulting from the diffusion of mature monomers  $\alpha = i + 1$ ,  $i = 0, 1, 2, \dots$ <sup>17</sup>.

In Figure 2 we show the convergence of iterates of equation (2), with  $P(a)$  given by equation (3). The limit satisfies the DFPE (1), and so is the form that we wish to compare to the scale-invariant GSD found in the MC simulations.

In Figure 3 we compare the numerically computed fixed points of equation (2), which we denote by  $\phi_\alpha(x)$ , with the GSDs of our MC simulations<sup>17</sup> for various critical island size  $i$ . The comparison is rather good. For  $i = 1, 2, 3$ , we see that the observed GSD lies between that of the  $\alpha = i + 1$  and  $\alpha = i$  distributional fixed point solutions. This can be expected since we have found elsewhere that island nucleation is driven by both deposition events and purely diffusional fluctuations in monomer density<sup>17</sup>. For spontaneous nucleation where  $i = 0$ , only

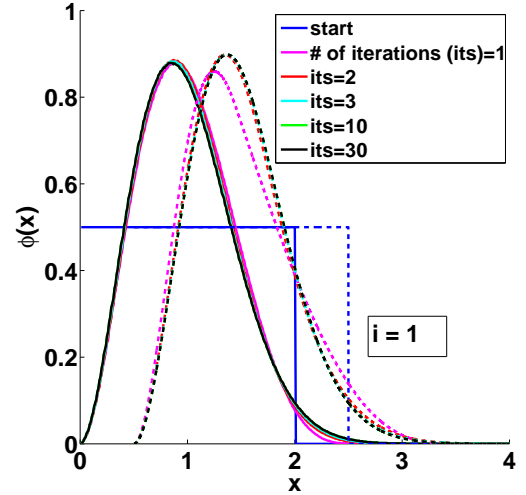


FIG. 2. The evolution of gap size distribution under iteration of equation (2) with  $i = 1$ . The solid lines are for  $\alpha = i + 1$  in equation (3), and the broken lines for  $\alpha = i$ , where the broken lines are shifted along the abscissa for clarity.

the  $\alpha = i + 1 = 1$  model is physically reasonable, since there is no possibility of a monomer depositing close to a pre-existing critical island of size  $i$  in this case.

It is interesting to ask how the solutions to the DFPE equation (2) compare to those of the forward-propagated fragmentation theory equations, for which the asymptotic behaviours are known<sup>14,15</sup>. As in [16], it can be shown that  $\phi_\alpha(x)$  obeys the delay-differential equation (DDE)

$$x^{2\alpha+1} \frac{d^{\alpha+1}}{dx^{\alpha+1}} \left[ \frac{\phi_\alpha(x)}{x^\alpha} \right] = \frac{(-1)^{\alpha+1} \alpha!}{B(\alpha + 1, \alpha + 1)} \phi_\alpha(x - 1), \quad (4)$$

from which it follows that

$$\phi_\alpha(x) \sim kx^\alpha \text{ as } x \rightarrow 0,$$

for some constant  $k$ . This is the same small-size asymptotic behaviour found in the fragmentation theory approach<sup>15,17</sup>. We could not obtain the large-size asymptotics for  $\phi_\alpha(x)$  from the DDE. However, numerical analysis of the solutions in Figure 3 show that they differ from those obtained by the fragmentation equation approach. The reason for this can be traced to the derivation of equation (1), where not only do we adopt a mean field approach for nearest neighbour gap sizes, but we also neglect longer-range correlations which are expected to be more prominent for larger gaps created early in the growth process. Nevertheless, the results in Figure 3 show that the solutions capture much of the essential physics for the GSDs.

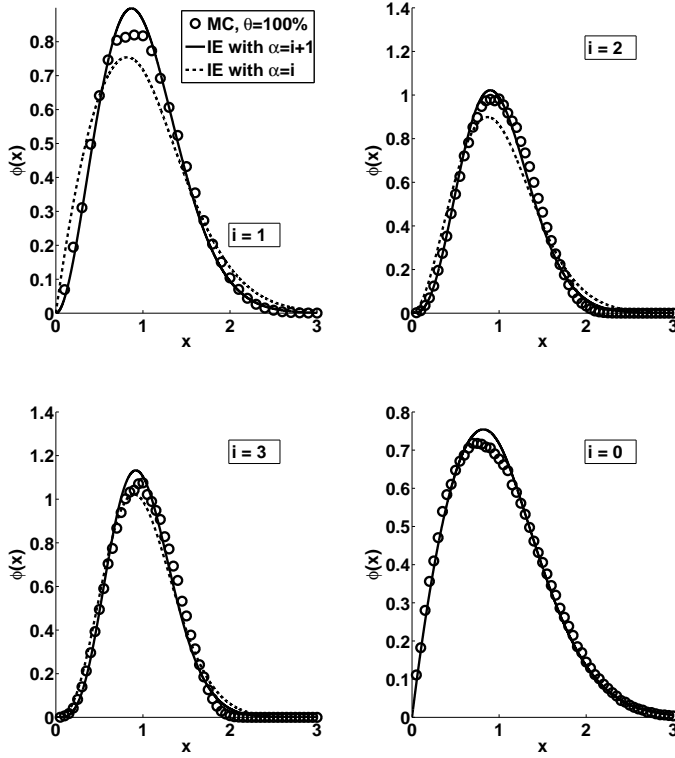


FIG. 3. The GSDs compared to histograms of MC data<sup>17</sup> for various critical island size  $i$ , taken at nominal coverage  $\theta = 100\%$  ( $\theta$  is deposition rate times elapsed time, and since we use point islands,  $\theta$  can be much larger than 1). The solid curves are the converged solutions to equation (2) with  $\alpha = i + 1$  with  $i = 0, 1, 2, 3$ , and the broken lines are for  $\alpha = i$  with  $i = 1, 2, 3$ .

We turn now to consider the evolution of the capture zones in the system. Referring back to Figure 1, we see that the capture zone  $C_5$  was created by the nucleation of island  $I_5$ . Prior to this, the zones  $C_3$  and  $C_4$  were larger, so that the creation of  $C_5$  can be viewed as the fragmentation of part of  $C_3$  (the part to the right of island  $I_3$ ) and part of  $C_4$  (to the left of  $I_4$ ). In general we do not know how much of the neighbouring capture zones to take, nor indeed how large these zones are. However, we can again invoke a mean field approximation for these nearest neighbour correlations to find the following DFPE for a general capture zone  $c$ :

$$c \triangleq \frac{1}{2}(a_1 + a_2)(1 + c). \quad (5)$$

The proportions  $a_1$  and  $a_2$  are independently drawn from  $P(a)$  of equation (3). An equivalent IE, like that of equation (2), can readily be identified for equation (5).

In Figure 4 we compare the Capture Zone Distributions (CZDs) obtained as fixed points of equation (5) with those from the MC simulations<sup>17</sup>. Again we find excellent agreement, particularly for  $i = 0$  and  $i = 1$ .

We also plot the Generalised Wigner Surmise (GWS) recently proposed<sup>18</sup> as a convenient analytical form for the CZDs whose only parameter depends solely on the critical island size  $i$ . We see that the solution of equation (5) fits the data at least as well as, and in the case of  $i = 0$  much better than, the GWS. Whilst the validity of the GWS has been questioned<sup>19,20</sup>, it is a useful benchmark for comparisons to MC data<sup>21,22</sup>.

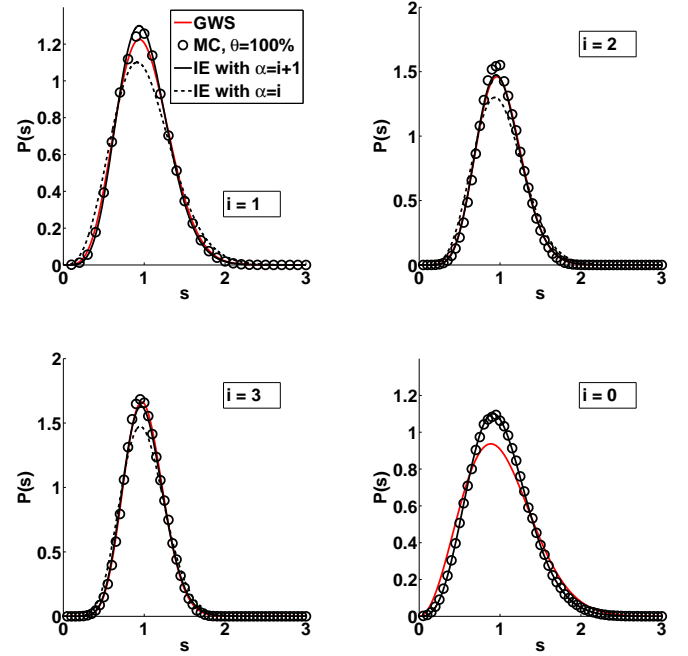


FIG. 4. The CZDs compared to histograms of MC data<sup>17</sup> for various critical island size  $i$ , taken at nominal coverage  $\theta = 100\%$ . The solid curves are the solutions to equation (5) for  $\alpha = i + 1$  with  $i = 0, 1, 2, 3$ , and the broken lines are for  $\alpha = i$  with  $i = 1, 2, 3$ .

We can easily quantify the performance of the solutions using the moments  $S_m$  of the distributions. Following [23], from equation (5) we find the following recursive relationship:

$$S_m = \left(\frac{1}{2}\right)^m \sum_{k=0}^m \frac{m!}{k!(m-k)!} B_{m-k} B_k \sum_{p=0}^m \frac{m!}{p!(m-p)!} S_p, \quad (6)$$

where

$$B_m = \frac{B(m + \alpha + 1, \alpha + 1)}{B(\alpha + 1, \alpha + 1)},$$

and  $B(m, n)$  is the Beta function as in Eqn. (3).

The moments of the GWS are given by

$$G_m = \frac{\Gamma(i + 3/2)^{m-1} \Gamma(i + (m + 3)/2)}{(i + 1)!^m}. \quad (7)$$

In Table I we compare the moments calculated from equations (6) and (7) alongside those taken from our MC simulations<sup>17</sup> for  $i = 0$  and  $i = 1$ . These confirm the superiority of the DFPEs, notably for  $\alpha = i + 1$  implying a greater significance for nucleation driven by monomer diffusion.

$m$	$i = 0$			$i = 1$			
	$G_m$	$S_m^a$	MC	$G_m$	$S_m^b$	$S_m^a$	MC
2	1.178	1.138	$1.134 \pm 0.001$	1.105	1.138	1.098	$1.098 \pm 0.001$
3	1.571	1.439	$1.425 \pm 0.001$	1.325	1.439	1.305	$1.307 \pm 0.001$
4	2.313	1.989	$1.949 \pm 0.001$	1.708	1.989	1.665	$1.666 \pm 0.001$

<sup>a</sup>  $\alpha = i + 1$

<sup>b</sup>  $\alpha = i$

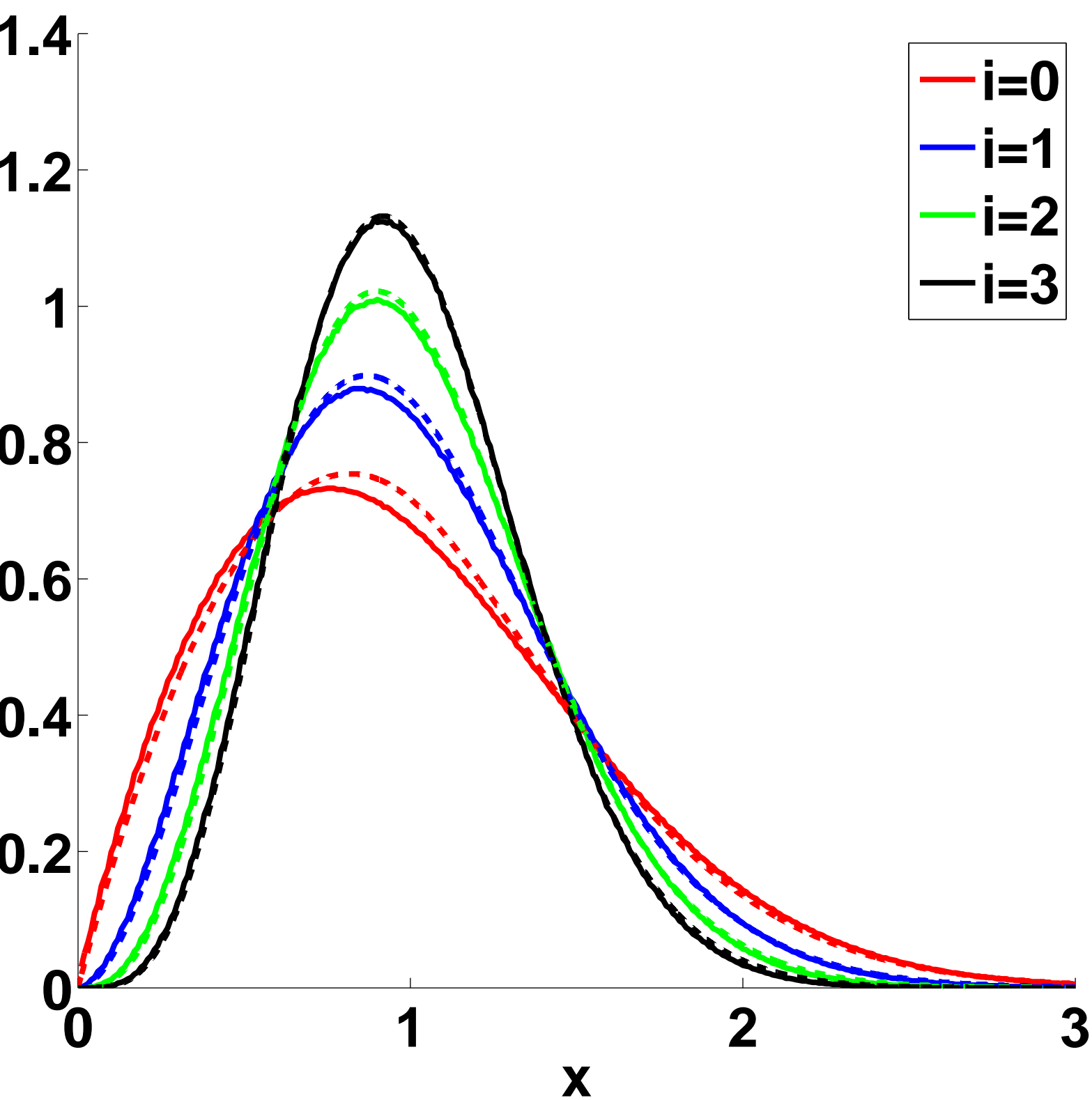
TABLE I. Moments of the CZDs from the GWS (equation (7), the distributional fixed point equations (equation (6) with  $\alpha = i + 1$  or  $\alpha = i$  if appropriate), and from the MC simulations<sup>17</sup> taken at  $\theta = 100\%$ .

In summary, we have presented distributional fixed point equations for the nucleation of point islands in one dimension. The approach develops a new retrospective view of how the inter-island gaps and capture zones have developed from the fragmentation of larger entities. That the resulting integral equations evolve to fixed points offers a new perspective on why scale-invariant distributions arise in the nucleation process. We have also shown that the solutions of our equations compare well to Monte Carlo simulation data<sup>17</sup>, performing at least as well as the recently proposed Generalised Wigner Surmise<sup>18</sup>, and notably better for the case of  $i = 0$ .

## ACKNOWLEDGMENTS

K.P.O is supported by the University of Strathclyde. The simulation data were obtained using the Faculty of Engineering High Performance Computer at the University of Strathclyde.

- <sup>1</sup>J. G. Amar and F. Family F, Phys. Rev. Lett. **74**, 2066 (1995).
- <sup>2</sup>P. A. Mulheran, Europhys. Lett. **65**, 379 (2004).
- <sup>3</sup>J. A. Venables, Philos. Mag. **27**, 693 (1973).
- <sup>4</sup>M. C. Bartelt and J. W. Evans, Phys. Rev. B **46**, 12675 (1992).
- <sup>5</sup>J. G. Amar, F. Family F and P. -M. Lam, Phys. Rev. B **50**, 8781 (1994).
- <sup>6</sup>G. S. Bales and D. C. Chrzan, Phys. Rev. B **50**, 6057 (1994).
- <sup>7</sup>J. A. Blackman and A. Wilding, Europhys. Lett. **16**, 115 (1991).
- <sup>8</sup>C. Ratsch, A. Zangwill, P. Smilauer, and D.D. Vvedensky, Phys. Rev. Lett. **72**, 3194 (1994).
- <sup>9</sup>P. A. Mulheran and J. A. Blackman Philo. Mag. Lett. (1995); P.A. Mulheran and J.A. Blackman, Phys. Rev. B **53**, 10261 (1996).
- <sup>10</sup>M. C. Bartelt and J. W. Evans, Phys. Rev. B **54**, R17359 (1996).
- <sup>11</sup>P. A. Mulheran and D. A. Robbie, Europhys. Lett. **49**, 617 (2000).
- <sup>12</sup>J. G. Amar, M. N. Popescu and F. Family, Phys. Rev. Lett. **86**, 3092 (2001).
- <sup>13</sup>J. W. Evans and M. C. Bartelt, Phys. Rev. B **66**, 235410 (2002).
- <sup>14</sup>J. A. Blackman and P. A. Mulheran, Phys. Rev. B **54**, 11681 (1996).
- <sup>15</sup>M. Grinfeld, W. Lamb, P. A. Mulheran and K. P. O'Neill, J. Phys. A **45**, 015002 (2012).
- <sup>16</sup>P. Seba, Acta Physica Polonica A **112**, 681 (2007).
- <sup>17</sup>K. P. O'Neill, M. Grinfeld, W. Lamb and P. A. Mulheran, Phys. Rev. E **85**, 021601 (2012).
- <sup>18</sup>A. Pimpinelli and T. L. Einstein, Phys. Rev. Lett. **99**, 226102 (2007).
- <sup>19</sup>F. Shi, Y. Shim and J.G. Amar, Phys. Rev. E **79**, 011602 (2009).
- <sup>20</sup>M. Li, Y. Han and J. W. Evans, Phys. Rev. Lett. **104**, 149601 (2010).
- <sup>21</sup>D. L. Gonzalez, A. Pimpinelli and T. L. Einstein, Phys. Rev. E **84**, 011601 (2011).
- <sup>22</sup>T. J. Oliveira and F. D. A. Araao Reis, Phys. Rev. B **83**, 201405 (2011).
- <sup>23</sup>M. Lallouache, A. Jedidi and A. Chakraborti, arXiv:1004.5109.



This figure "paul.jpg" is available in "jpg" format from:

<http://arxiv.org/ps/1202.5327v1>